



# Numerical analysis of a slope stabilized with piles and anchor cable frame beams

Changcheng Du<sup>1</sup> · Jianfeng Chen<sup>1,2</sup> · Sixian Chen<sup>3</sup> · Ming Peng<sup>1,2</sup> · Zhenming Shi<sup>1,2</sup>

Received: 20 April 2022 / Accepted: 24 January 2023 / Published online: 8 February 2023  
© The Author(s), under exclusive licence to Springer-Verlag GmbH Germany, part of Springer Nature 2023

## Abstract

A landslide located in northern Sichuan Province, China was investigated. A series of numerical models of the landslide stabilized with piles and anchor cable frame beams were developed using a three-dimensional finite-element method. The Strength Reduction Method was employed to investigate the stability of slopes, the internal forces of piles, and the axial forces of anchor cables. A parametric study consisting of pile position, pile length, and pile spacing was carried out. The results show that compared to anchor cable frame beams, the combination of piles and anchor cable frame beams is a more effective retaining structure to improve slope stability. During slope destabilization, the proportion of thrust shared by piles gradually increases, while the proportion of thrust shared by anchor cables gradually decreases. Piles installed on the leading edge of a trail-mode landslide can make the slope mostly stable. As the piles move from the leading, middle, and trailing edges of the slope, the proportion of thrust shared by the anchor cables gradually increases, while local instability may occur in front of the pile. Increasing the pile length can improve the stability of the slope. However, excessive embedded length of piles has little effect on further improving the slope stability. The critical embedment length of piles found in this study is 1/3 of the total length of the pile. The critical pile spacing found in this study is 2.5 times the width of the pile section. Beyond this spacing, the effective soil arch between the piles is difficult to develop and the anchor cables may share more proportion of the landslide thrust. This study provides a reference for reinforcement system design of engineering projects considering piles and anchor cable frame beams.

**Keywords** Slope · Pile · Anchor cable frame beam · Numerical model

## Introduction

Retaining structures are crucial for slope stabilization. In particular, piles owning excellent anti-slip capability can prevent the overall instability of the slope (Li et al. 2016; Xiao et al. 2017; Zhao et al. 2017, 2019; Wang et al. 2021a, b). Anchor cable frame beams are also a key retaining structure, which can restrain the surface deformation of slopes rapidly by applying pre-stresses to the unstable slope (Chen et al. 2016, 2018). In mountainous areas, slope conditions are commonly complicated. A single retaining structure is unlikely to be successful in controlling large-scale landslides, thus more and more combination structures were proposed (Zhang et al. 2020; Feng et al. 2021; Wang et al. 2021a, b). The combined structure of piles and anchor cable frame beams (CPA) can ensure both global and local stability of the slope, which is widely used in various landslide control projects (Lin et al. 2017; Xue et al. 2018).

---

✉ Jianfeng Chen  
jf\_chen@tongji.edu.cn  
Changcheng Du  
duchangcheng@tongji.edu.cn  
Sixian Chen  
1832665@tongji.edu.cn  
Ming Peng  
pengming@tongji.edu.cn  
Zhenming Shi  
shi\_tongji@tongji.edu.cn

<sup>1</sup> Department of Geotechnical Engineering, Tongji University, Shanghai 200092, China  
<sup>2</sup> Key Laboratory of Geotechnical and Underground Engineering, Ministry of Education, Shanghai 200092, China  
<sup>3</sup> Fuzhou Planning and Design Research Institute Group Co., Ltd, Fuzhou 350108, China

Piles are passive retaining structures, which only come into play when the slope starts to deform (Kahyaoglu et al. 2017; Li and Du 2021). The reasonable pile position, pile length, and pile spacing are the main factors affecting the effect of slope reinforcement (Xiao 2017; Tan et al. 2018; Liu et al. 2018; Li et al. 2019). For the pile position, Ito et al. (1981) and Hassiotis et al. (1997) concluded that the factor of safety ( $FS$ ) was maximum for slopes with piles installed at the top of the slope. However, Shooshpasha and Amirdehi (2015) derived that the  $FS$  was maximum for piles installed in the middle of the slope. Similarly, Wei and Cheng (2009) suggested that the optimal location of the pile is near the middle of the slope. For the pile length, Cai and Ugai (2000) suggested that the slip surface of the slope no longer changed for pile length exceeding the critical value. However, Griffiths and Marquez (2007) noted that the slip surface may become shallow for a pile whose length exceeds a certain threshold value. Additionally, there is also no consensus on the issue of optimal pile spacing owing to the presence of earth arches between piles (Cai and Ugai 2000; Wei and Cheng 2009).

Anchor cable frame beams are active retaining structures, which can be employed simultaneously with piles to develop a combined structure (Wu and Huang 2008; Lin et al. 2017; Xue et al. 2018). For this combined structure, piles and anchor cables share the landslide thrust to maintain the stability of the slope. However, its force mechanisms are usually complex due to the coordinated deformation of the active and passive structures. Compared to the research on pile-stabilized slopes, there are few studies about the slope stabilized with piles and anchor cable frame beams. Li and Wang (2016) conducted field tests on a slope stabilized with the CPA. Their results showed that the anchor cables and the piles work in concert, sharing 33.9% and 66.1% of the thrust, respectively. However, the proportion of thrust shared by piles and anchor cables is also related to their location and number, which requires further research to clarify.

A landslide located in northern Sichuan Province, China, was investigated. A series of numerical models of a slope stabilized with piles, and anchor cable frame beams were developed using a three-dimensional finite-element method. The Strength Reduction Method (SRM) was employed to investigate the stability of slopes, the internal forces of piles, and the axial forces of anchor cables. A parametric study consisting of pile position, pile length, and pile spacing was carried out.

## Project description

### Landslide on a slope stabilized with anchor cable frame beams

The slope is located in northern Sichuan Province, China. The strata are, from top to bottom, pebbly silty clay, strongly weathered argillaceous shale, moderately weathered argillaceous shale, and moderately weathered silty shale. In March 2013, the slope was excavated at an elevation of 606–706 m, with an extent of approximately 260 m in length and 170 m in width. The anchor cable frames were adopted in the original scheme, as shown in Fig. 1. The length of the anchor cable is 17–26 m, the anchorage length is 8.5 m, the horizontal spacing is 2.0–3.0 m, the vertical spacing is 2.0–2.5 m, and the pre-stress value is 500 kN. The cross-sectional dimension of the frame beam is 0.4 m × 0.45 m.

In July 2014, a landslide occurred. The overview of the landslide is shown in Fig. 2. The landslide is shown in the shape of a lap chair in the aerial view. The volume of the landslide is approximately 478,000 m<sup>3</sup>. The main slip direction of the landslide is 347°. The plan of the landslide is shown in Fig. 3.

The site investigation showed that the landslide was mainly caused by excavation at the foot of the slope. Thus, it is a trail-mode landslide. Another cause of the landslide was the short length of the anchor cables in the original

**Fig. 1** Section of the slope stabilized with the original scheme

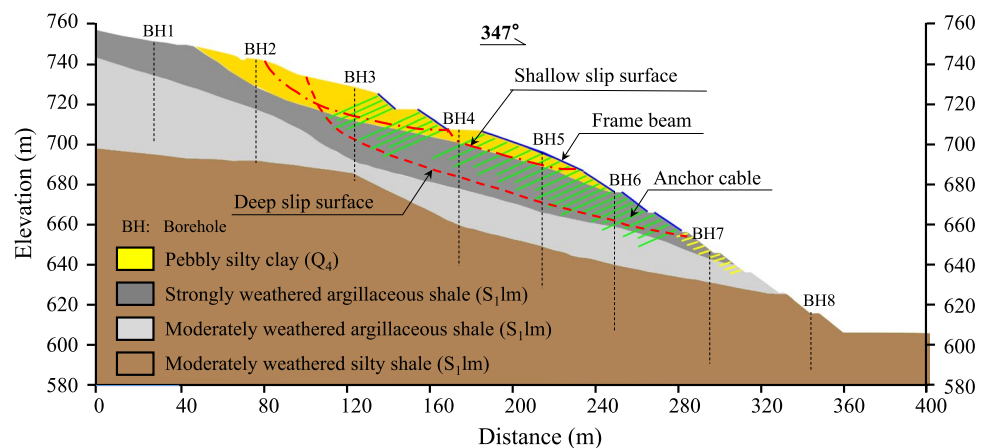


**Fig. 2** Overview of the landslide

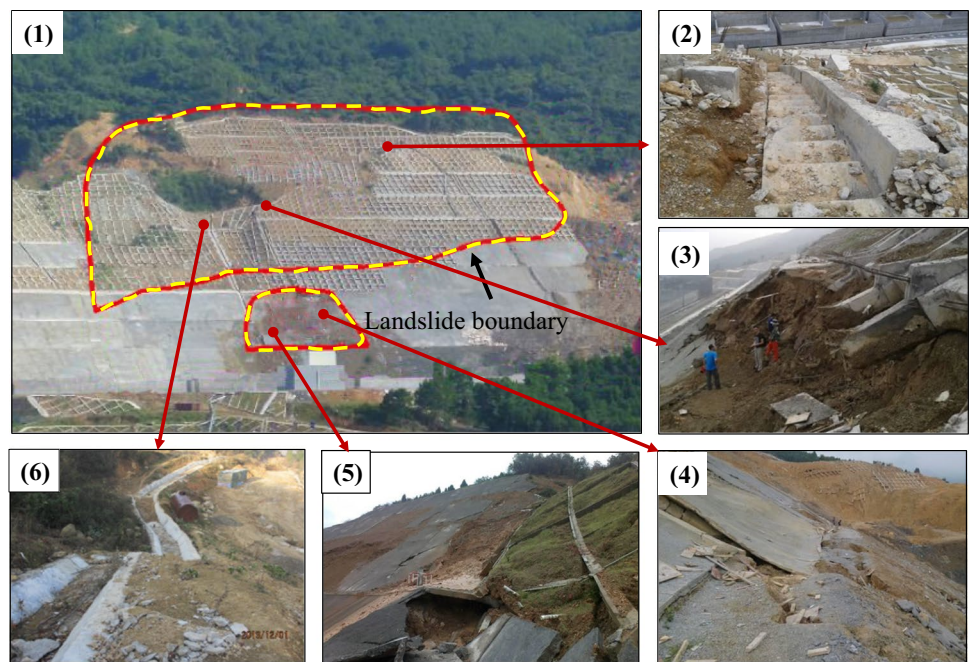
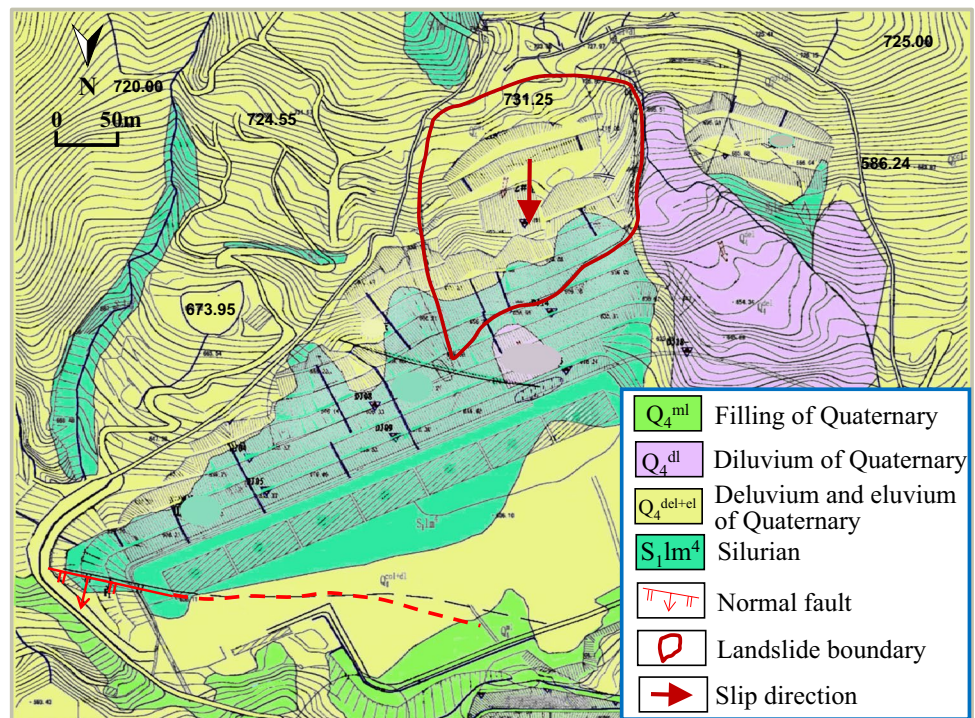


**Fig. 3** Plan of the landslide

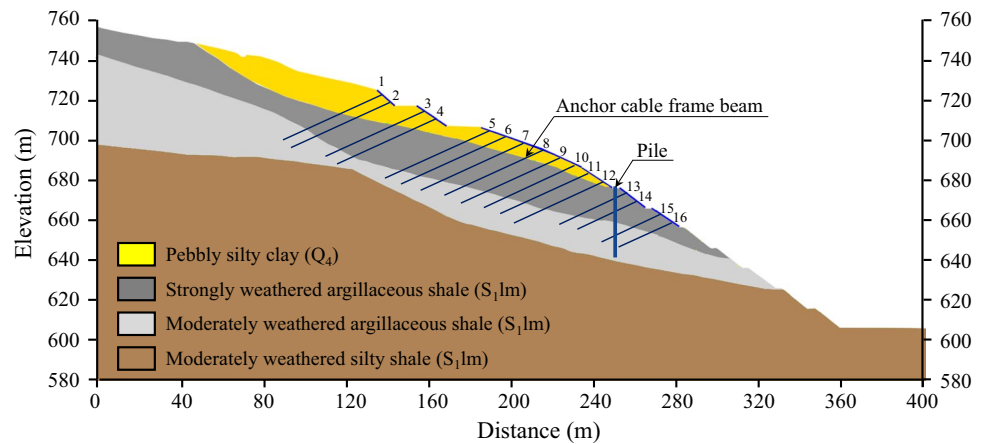


scheme. The anchor cables were installed in strongly weathered argillaceous shale, which allows the slip surface to bypass the end of the anchor cables.

**Scheme for piles and anchor cable frame beams**

The landslide was then stabilized with a CPA scheme, as shown in Fig. 4. Piles with a cross-section of  $2 \times 3$  m, a spacing of 5 m, and a length of 35 m were installed at the

**Fig. 4** Scheme of piles and anchor cable frame beams



leading edge of the landslide. Anchor cables with a length of 35–60 m, a horizontal spacing of 2.5 m, a vertical spacing of 3 m, an anchorage length of 8 m, and an anchorage angle of  $25^\circ$  were provided. It is worth mentioning that the anchor cables were anchored in moderately weathered argillaceous shale and the length of the anchor cable was increased compared to the original scheme.

## Numerical model

### Overview

A three-dimensional finite-element program was employed to develop numerical models of the slopes for the original and CPA schemes, as shown in Fig. 5. The dimensions of the model were  $395\text{ m} \times 10\text{ m} \times 176\text{ m}$  (length  $\times$  width  $\times$  height). The number of grids was approximately 70,000. One-dimensional units and three-dimensional units were selected to build the anchor cables and the piles, respectively. The constitutive model for the slope and structural elements were Mohr–Coulomb and Elastic, respectively. Tables 1, 2 and 3 show the parameters for the slope, piles, and anchor cables, respectively. The saturation values were adopted for the strength parameters in this model. It is important to note that some of the material parameters were obtained from the field and laboratory and partly were based on empirical assumptions.

### Validation of the finite-element model

The SRM is adopted frequently for calculating the stability of reinforced slopes (Lin et al. 2013; Rawat and Gupta 2016; Arvin et al. 2019). Thus, the SRM was employed to calculate the *FS* for the original scheme and the CPA scheme. The *FS* for the original scheme is 1.025, which is close to the ultimate failure state. Figure 6 shows the equivalent plastic strain contour of the slope stabilized with the original scheme. The

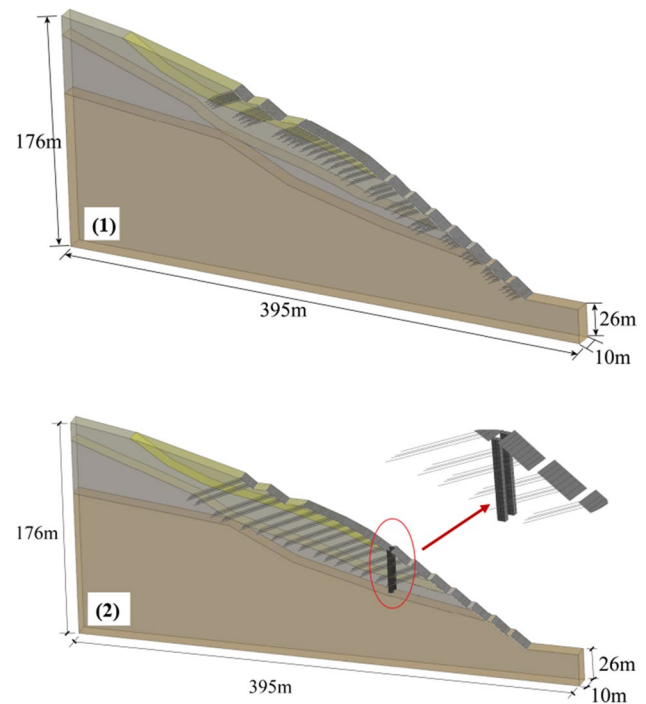


**Fig. 5** Numerical model: (1) original scheme and (2) CPA scheme

potential slip surface bypasses the end of the anchor cables. The shape and location of the slip surface are consistent with the results of the site investigation. Additionally, the maximum equivalent plastic strain is at the leading edge of the landslide; thus, it is a trail-mode landslide. Again, it is consistent with the results of the site investigation. Therefore, the numerical model developed in this study is acceptable.

**Table 1** Parameters of the slope in the numerical model

Material	Constitutive model	$\gamma$ (kN m <sup>3</sup> )	$E$ (MPa)	$\nu$	$\phi$ (°)	$c$ (kPa)
Pebbly silty clay	MC	19	24	0.35	15.5	23
Strongly weathered argillaceous shale	MC	21	65	0.3	19	46
Moderately weathered argillaceous shale	MC	23.5	450	0.25	29	120
Moderately weathered silty shale	MC	23.5	1800	0.25	35	298

MC Mohr–Coulomb,  $\gamma$  unit weight,  $E$  Young’s modulus,  $\nu$  Poisson’s ratio,  $\phi$  friction angle,  $c$  cohesion

**Table 2** Parameters of the pile in the numerical model

Material	Constitutive model	$\gamma$ (kN m <sup>3</sup> )	$E$ (MPa)	$\nu$	$E_n$ (MPa)	$E_t$ (MPa)
Pile	Elastic	24	30,000	0.2	1800	200

$E_n$  normal contact stiffness,  $E_t$  tangential contact stiffness

**Table 3** Parameters of the anchor cable in the numerical model

Material	Constitutive model	$\gamma$ (kN m <sup>3</sup> )	$E$ (MPa)	$\nu$	$T_{ult}$ (kN)
Anchor cable	Elastic	78	195,000	0.2	1350

$T_{ult}$  ultimate pull-out resistance

stability of the slope. The maximum equivalent plastic strain occurs at the leading edge of the potential slip surface, which suggests that the potential trail-mode landslide may have occurred on the slope.

### Internal force of piles and axial force of anchor cables

The SRM was employed to investigate the internal forces of piles and the axial forces of anchor cables for different reduction factors ( $k = 1.00, 1.05, 1.10, 1.15, 1.20,$  and  $1.24$ ). Figure 8 shows the diagram of bending moment and shear force of piles for different reduction factors. The bending moment of the pile is S-shaped. The bending moment at 20 m from the pile head is zero. Above this depth, the pile has a negative bending moment and vice versa. The maximum values

## Results and analysis

### Stability of slope

Figure 7 shows the equivalent plastic strain contour of the slope stabilized with the CPA scheme. The  $FS$  of the CPA scheme is 1.240. Anchor cables and piles pass through the potential slip surface. The CPA scheme ensures the

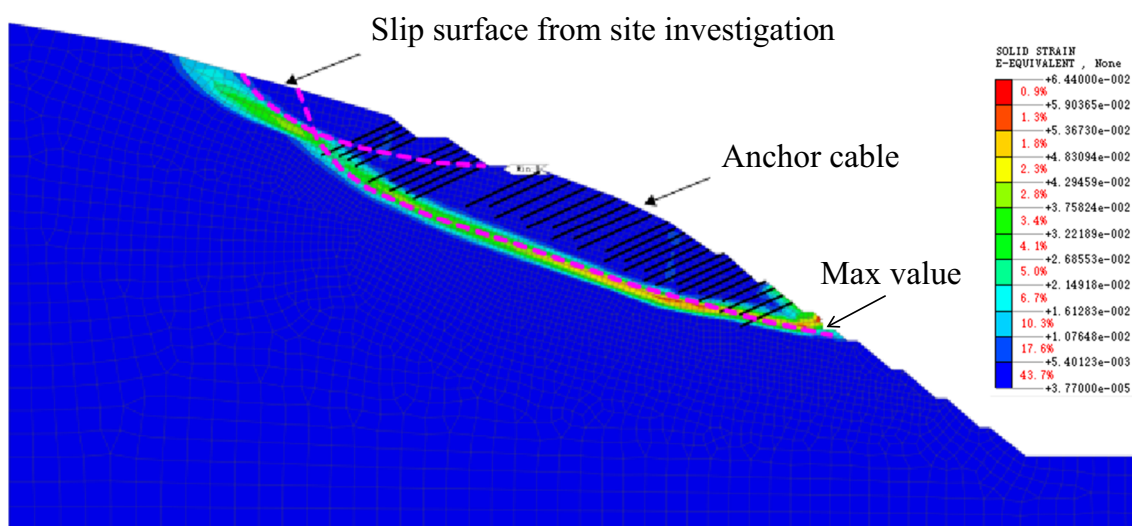


**Fig. 6** Equivalent plastic strain contour of the slope stabilized with the original scheme

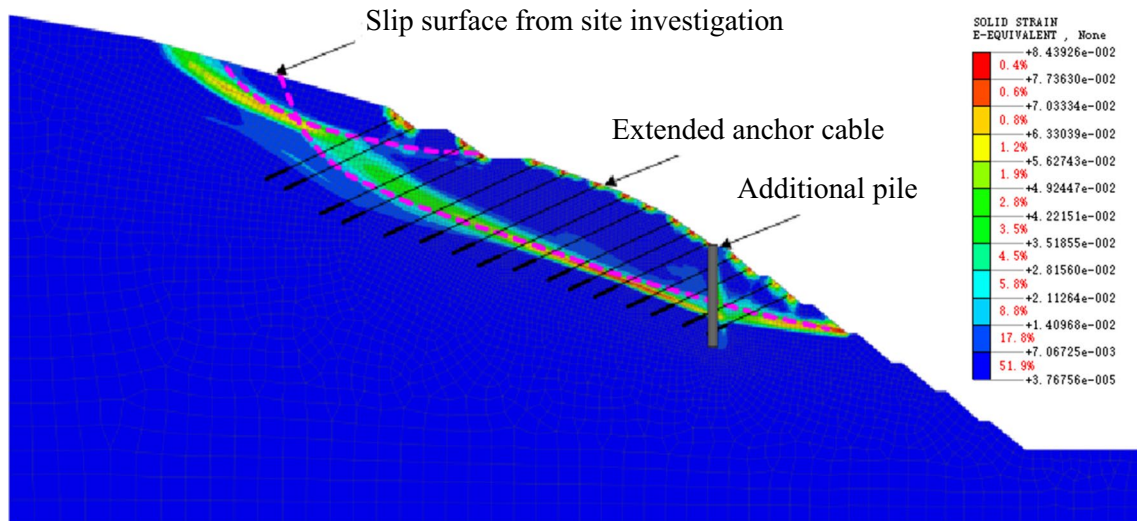
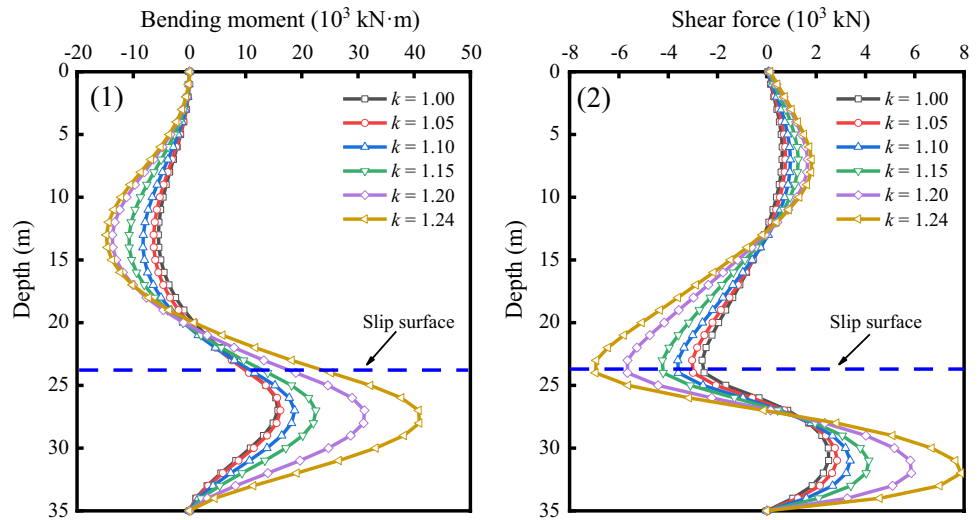


Fig. 7 Equivalent plastic strain contour of the slope stabilized with the CPA scheme

Fig. 8 Diagram of internal force of piles: (1) bending moment and (2) shear force



of the negative and positive bending moments occur at a depth of about 13 m and 27 m from the pile head, respectively. The shape of the bending moment remains the same, but its value gradually increases as the reduction factor increases. The increase in the positive bending moment is significantly greater than the increase in the negative bending moment. Additionally, the maximum shear force occurs near the slip surface, approximately 24 m (17/25 of the total length) from the pile head, which is also observed for real piles in practical engineering (Kang et al. 2009). The shape of the shear forces remains the same, but its value gradually increases as the reduction factor increases.

Poulos (1995) suggested that the ‘intermediate mode’ allows the pile to provide maximum anti-slip resistance. At this point, the bending moment of the pile is S-shaped and

the depth of the slip surface is 3/5–7/10 of the total length. The internal forces of the piles in this study are consistent with the ‘intermediate mode’, indicating that the configuration of the piles is reasonable.

Figure 9 shows the axial forces of anchor cables for different reduction factors ( $k = 1.00, 1.05, 1.10, 1.15, 1.20,$  and  $1.24$ ). The anchor cables are numbered, as shown in Fig. 4. The anchor cables installed in the lower part of the slope have a relatively high axial force. This is attributed to the fact that this slope is a trail-mode landslide and the deformation in its lower part is greater. In addition, the axial force of the anchor cables increases with the increased reduction factor. Anchor cables 15 and 16 were pulled out when the reduction factor increases to 1.24. Thus, more anchor cables

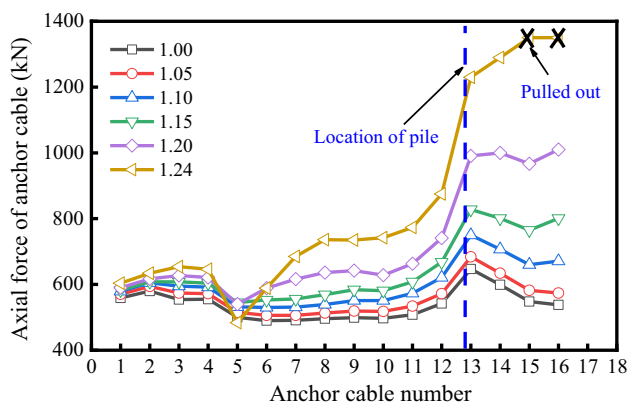


Fig. 9 Axial force of anchor cables for different reduction factors

may be pulled out from the leading edge of the slope when the stability of the slope is further reduced.

Figure 10 shows the calculation diagram of the thrust shared by piles and anchor cables. The thrust shared by piles,  $F_p$ , is the component of the shear force  $Q$  of the pile on the slip surface in the tangential direction of the slip surface, calculated according to Eq. (1)

$$F_p = \frac{1}{D} Q \cos \theta, \tag{1}$$

where  $D$  is the pile spacing;  $\theta$  is the angle between the tangential direction of the slip surface and the horizontal direction.

The axial force  $N_i$  of anchor cables can be decomposed into a normal force  $T_{i1}$  and a tangential force  $T_{i2}$ . The thrust shared by anchor cables,  $F_c$ , is the sum of the frictional force generated by the normal force  $T_{i1}$  and the tangential force  $T_{i2}$ , calculated according to Eqs. (2)–(4)

$$T_{i1} = N_i [\sin (\alpha_i + \beta_i)], \tag{2}$$

$$T_{i2} = N_i [\cos (\alpha_i + \beta_i)], \tag{3}$$

$$F_c = \frac{1}{S} \sum [T_{i2} + T_{i1} \tan \varphi], \tag{4}$$

where  $\alpha_i$  is the angle between the slip surface and the horizontal direction at the  $i$ th row of anchor cables;  $\beta_i$  is the angle between the  $i$ th row of anchor cables and the horizontal direction;  $S$  is the horizontal spacing between anchor cables; and  $\varphi$  is the internal friction angle of the slip surface.

The proportion of the thrust shared by piles and anchor cables for different reduction factors can be obtained according to Eqs. (1)–(4), as shown in Fig. 11. When the reduction factor  $k$  is increased from 1.0 to 1.24, the proportion of thrust shared by the pile increases from 16.2 to 30.3%, while the proportion of thrust shared by the anchor cable decreases from 83.7 to 69.7%. The piles and anchor cables show a synergistic working effect.

Because the landslide thrusts are shared by the piles and anchor cables, designers often roughly distribute the

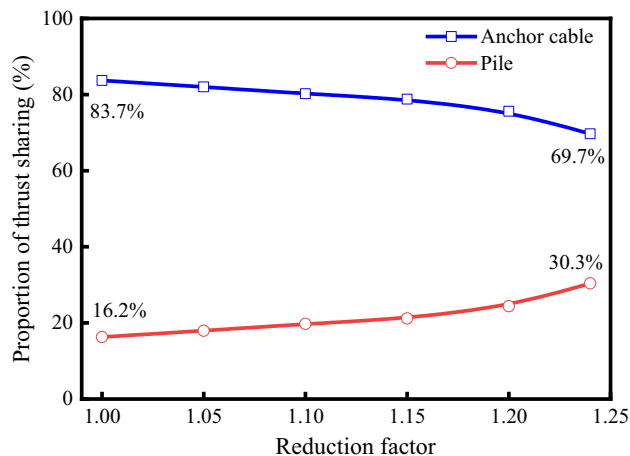
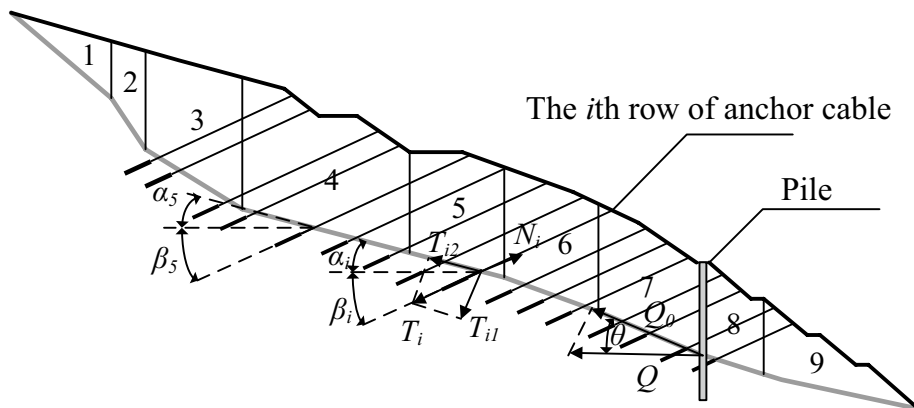


Fig. 11 Proportion of the thrust shared by piles and anchor cables for different reduction factors

Fig. 10 Calculation diagram of the thrust shared by piles and anchor cables



thrust between the pile and the anchor cables in practice. However, the proportion of thrust shared by piles and anchor cables varies during slope deformation. Anchor cables are the main thrust-bearing structure at the initial stage, whereas the piles start to share more of the thrust only when the slope slips. Additionally, the proportion of thrust shared by piles or anchor cables is also related to the relative number of piles and anchor cables. In the case of this study, the piles shared 16.2% of the total thrust for a row of piles and 16 rows of anchor cables installed on the slope. In contrast, in the findings of Li et al. (2016), the piles shared 66.1% of the total thrust for a row of piles and two rows of anchor cables installed on the slope. Therefore, the proportion of the thrust shared by piles or anchor cables is not recommended to be artificially specified in the engineering design.

## Parametric studies

### Effect of pile position

Four different pile positions were considered, as shown in Table 4. The piles were installed at the leading edge of the slope (Pile 1), the middle front edge of the slope (Pile 2), the middle back edge of the slope (Pile 3), and the

trailing edge of the slope (Pile 4), respectively, as shown in Fig. 12.

### Stability of slope

Figure 13 shows the equivalent plastic strain contours of the slope without piles and with different pile positions. Local failure of the slope in front of the piles occurs as the piles gradually move toward the trailing edge of the slope. The extent of the local failure gradually remains constant for the piles approaching the trailing edge of the landslide. This indicates that piles installed at the leading edge of the trail-mode landslide can avoid the local instability of the slope.

Figure 14 shows the *FS* of the slope with different pile positions. The *FS* of the slope without pile is 1.141. The *FS* of the slope stabilized with piles has been improved. Compared to the without pile case, the *FS* of the slope for Pile 1, Pile 2, Pile 3, and Pile 4 is increased by 10.4%, 3.3%, 0.6%, and 0.2%, respectively. This indicates that the slope where the piles are installed on the leading edge has the greatest stability, which is because the pile installed at the trailing edge of the trail-mode landslide can avoid the local instability of the slope, as shown in Fig. 13.

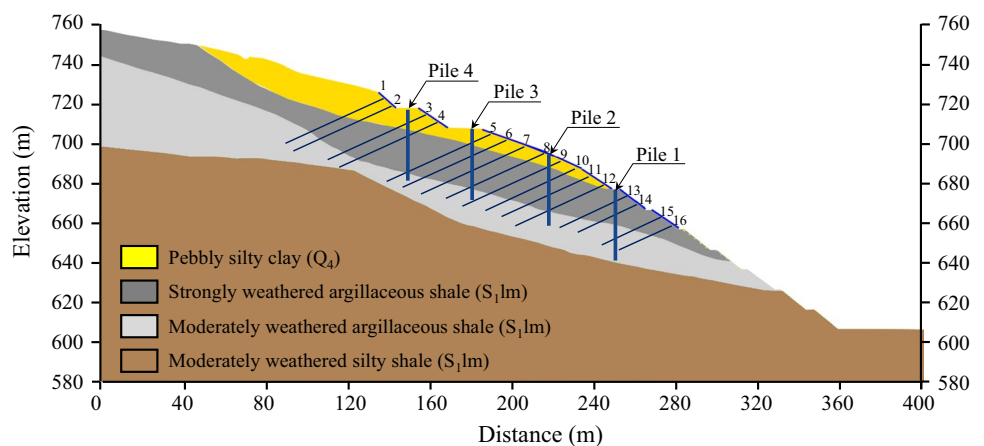
### Internal force of piles and axial force of anchor cables

Figure 15 shows the diagram of bending moment and shear forces of piles for different pile positions. The maximum bending moment of the piles gradually decreases as the piles move toward the trailing edge of the slope. The maximum positive shear forces of the piles for all pile positions are located below the slip surfaces, while the maximum negative shear forces are located near the slip surface. Both the maximum positive and negative shear forces gradually decrease from Pile 1 to Pile 4. This reveals that the closer the piles are to the trailing edge of the slope, the less the landslide thrust the piles will be subjected to.

**Table 4** Calculation schemes of four different pile positions

Scheme	Pile position	Pile length (m)	Pile spacing (m)
1	Pile 1	40	5
2	Pile 2	40	5
3	Pile 3	40	5
4	Pile 4	40	5

**Fig. 12** Diagram of four different pile positions





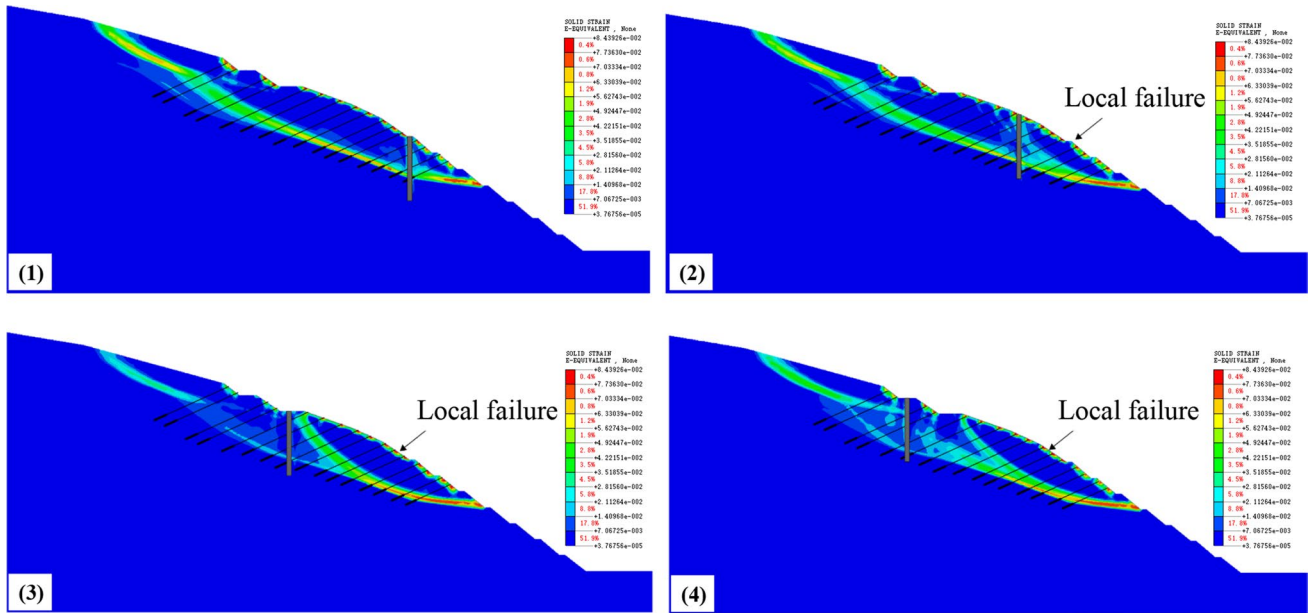


Fig. 13 Equivalent plastic strain contours of slopes with different pile positions: (1) Pile 1; (2) Pile 2; (3) Pile 3; and (4) Pile 4

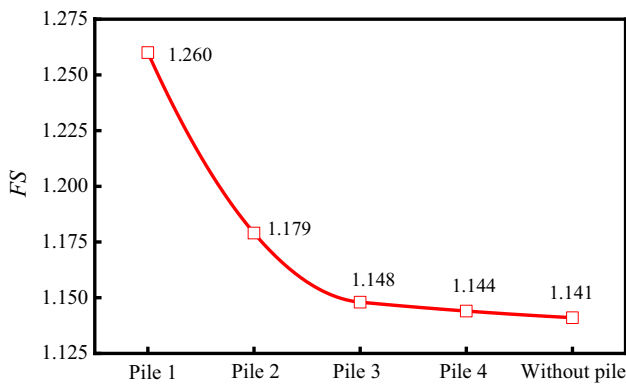
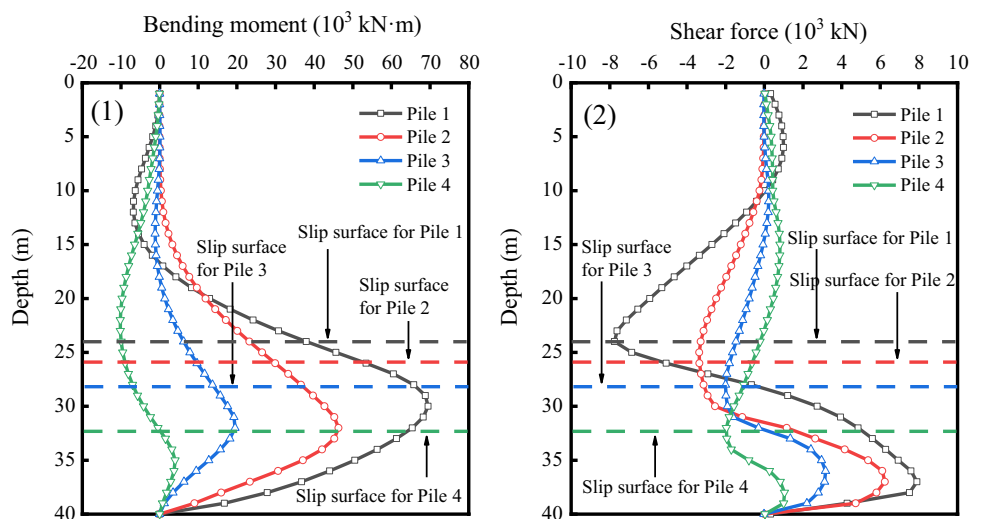


Fig. 14 FS of slopes with different pile positions

Figure 16 shows the axial force of anchor cables for different pile positions. The axial force of the anchor cables installed in the lower part of the slope is significantly greater than those installed in the upper part. The axial force of the anchor cables in front of the piles increases significantly with the piles moving from Pile 1 to Pile 3. However, the axial force of the anchor cables behind the piles does not change much. This is because the piles cannot provide slip resistance to the slope in front of them.

Figure 17 shows the proportion of thrust shared by piles and anchor cables for different pile positions. When piles move from Pile 1 to Pile 3, the proportion of thrust shared by

Fig. 15 Diagram of internal force of piles for different pile positions: (1) bending moment and (2) shear force



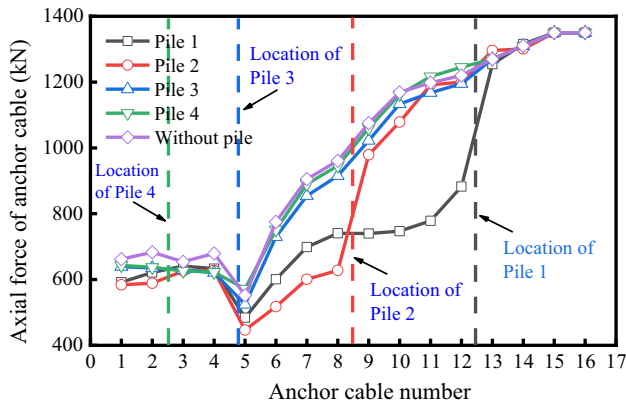


Fig. 16 Axial force of anchor cables for different pile positions

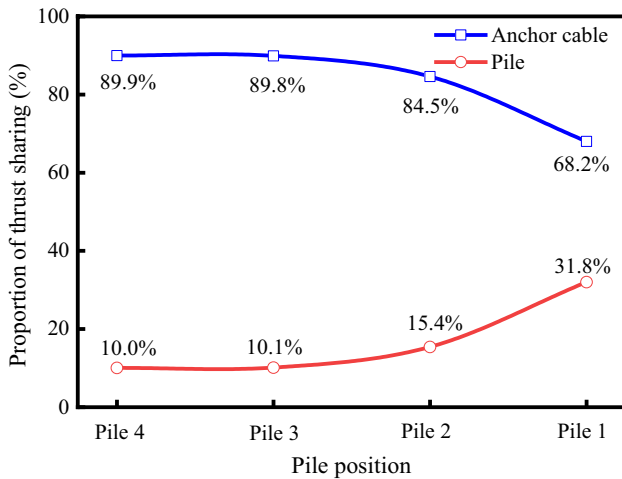


Fig. 17 Proportion of the thrust shared by piles and anchor cables for different pile positions

the pile decreases from 31.8 to 10.1%, while the proportion of thrust shared by the anchor cable increases from 68.2 to 89.9%. However, when piles move from Pile 3 to Pile 4, the proportion of thrust shared by the pile and the anchor cable remains almost constant.

As described by Xue et al. (2018), installing piles at the foot of the slope can maintain the stability of the excavated slope. For potential trail-mode landslides, more of the landslide thrust can be shared by the passive piles installed at the leading edge of the slope. However, the initial deformation location of a push-mode landslide differs from that of a trail-mode landslide. In practice, the optimal pile position thus should be chosen according to the potential slip mode of the slope. Such as piles should be installed at the leading edge of trail-mode landslides or the trailing edge of push-mode landslides.

Table 5 Calculation schemes for different pile lengths

Scheme	Pile position	Pile length (m)	Pile spacing (m)
1	Pile 1	20	5
2	Pile 1	25	5
3	Pile 1	30	5
4	Pile 1	35	5
5	Pile 1	40	5

### Effect of pile length

Five different pile lengths were considered, as shown in Table 5. To determine the critical values of embedment length, a wide range of the parameter is initially selected referring to the Specification of design and construction for landslide stabilization (DZ/T 0219-2006) and the code for the design of landslide stabilization (GB/T 38509-2020). The pile length is set to 20 m, 25 m, 30 m, 35 m, and 40 m, respectively. Other parameters remain unchanged.

### Stability of slope

Figure 18 shows the equivalent plastic strain contours of the slope for different pile lengths. The contour for the piles with a length of 40 m is shown in Fig. 13(1). For pile lengths of 20 m, 25 m, and 30 m, the embedment length is 0–1/5 of the pile length and the potential slip surface crosses the bottom of the piles. For pile lengths of 35 m and 40 m, the embedment length is 1/3–2/5 of the pile length, and the piles intersect with the potential slip surfaces. This indicates that the piles lose their anti-slip capacity when the embedded length of piles is insufficient.

Figure 19 shows the *FS* of the slope for different pile lengths. The *FS* of the slope for the pile length of 20 m is 1.154. The *FS* gradually increases with the increased pile length. Compared to the pile length of 20 m, the *FS* of the slope for pile lengths of 25 m, 30 m, 35 m, and 40 m is increased by 0.5%, 1.5%, 8.0%, and 9.1%, respectively. This indicates that the *FS* increases dramatically when the pile length increases from 30 to 35 m, while it increases slowly when the pile length is less than 30 m. The above results can be explained by the relationship between the piles and the slip surfaces in Fig. 18. The piles intersect with the slip surfaces for piles with an embedment length greater than 1/3 of the total length. In contrast, they contribute little to the stability of the slope when the piles are located above the slip surface. Additionally, the *FS* increases slowly when the pile length is longer than 35 m, which indicates that excessive embedded length of piles has little effect on further improving the slope stability.

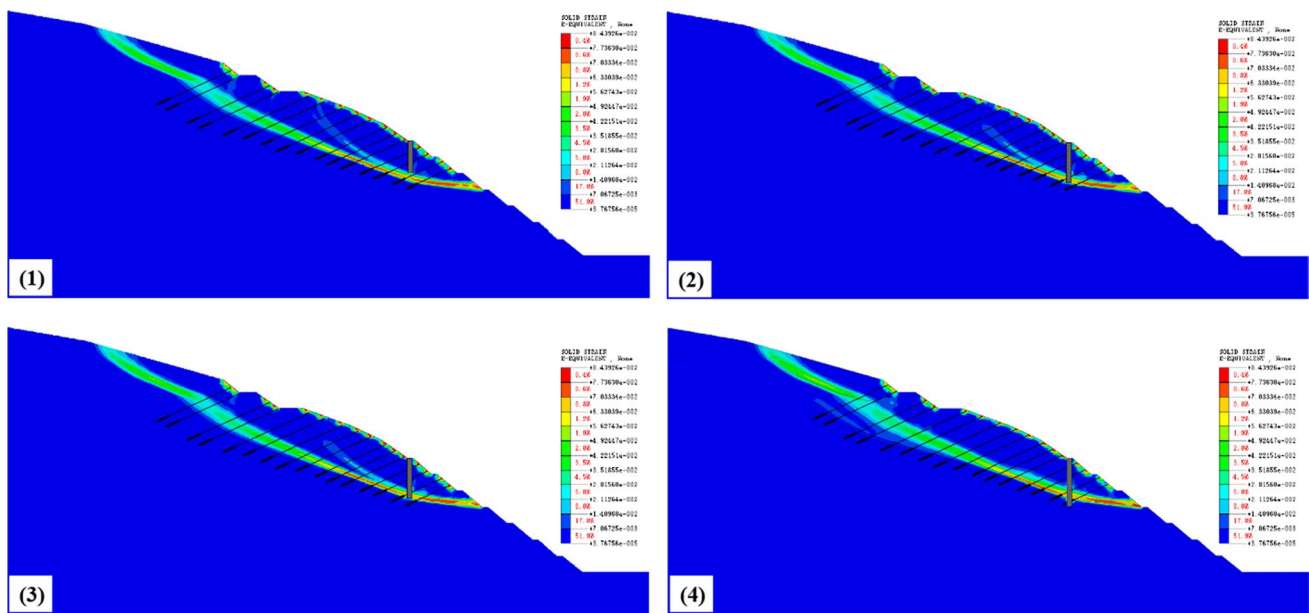


Fig. 18 Equivalent plastic strain contours of slopes for different pile lengths: (1) 20 m; (2) 25 m; (3) 30 m; and (4) 35 m

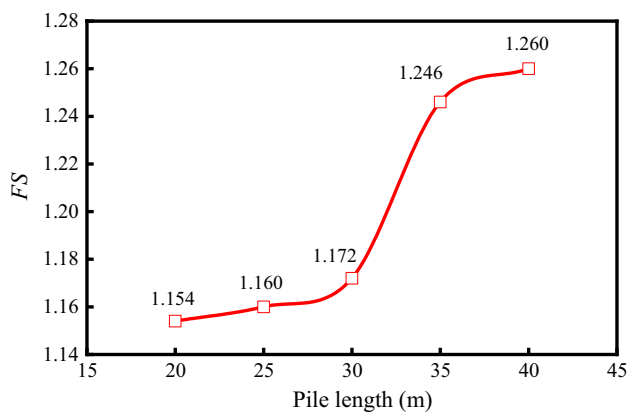


Fig. 19 FS of slopes for different pile lengths

**Internal force of piles and axial force of anchor cables**

Figure 20 shows the diagram of the bending moment and shear force of the pile for different pile lengths. The maximum bending moment of the pile is above the slip surface for pile lengths of 20 m, 25 m, and 30 m. The maximum bending moment of the pile is below the slip surface for pile lengths of 35 m and 40 m. As the pile length increases from 30 to 35 m, the maximum bending moment of the pile changes from negative to positive by approximately 2100%. After that, as the pile length continues to increase, the shape of the bending moment of the pile no longer changes. However, the maximum bending moment increases from 41,023 kN·m at 35 m to 69,480 kN·m at 40 m, approximately 69%.

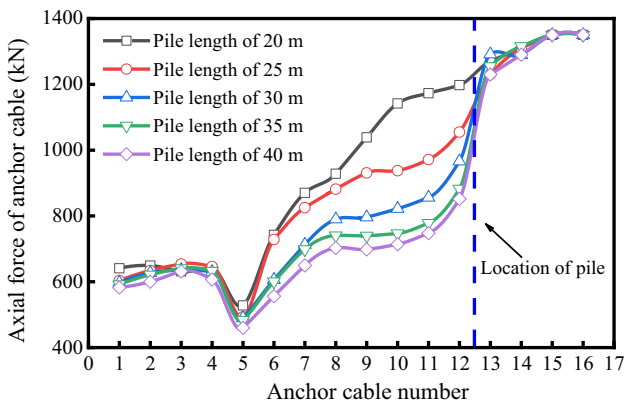
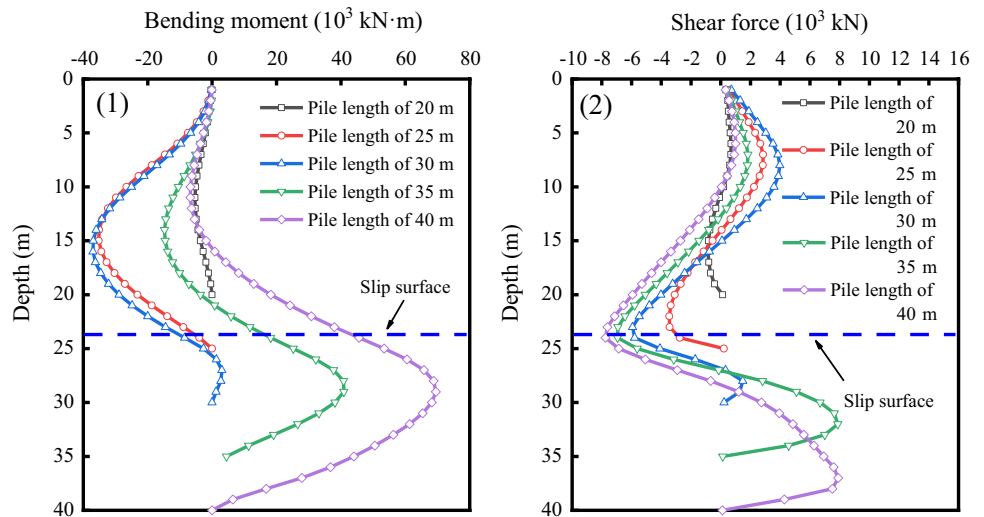
For pile lengths of 25 m and 30 m, the maximum shear force of the pile occurs near the slip surface. When the length of the pile is 35 m, the peak of the shear force also appears in the middle of the pile in the soil. When the pile length is 40 m, the shape and the maximum value of the shear force of the pile no longer change significantly. This indicates that the landslide thrust borne by the pile increases and the pile exerts its anti-slip effect when the length of the pile exceeds 35 m. The reason for this result is consistent with that for the FS in "Stability of slope".

Figure 21 shows the axial force of anchor cables for different pile lengths. The axial force of anchor cables in the middle of the slope decreases significantly with increased pile lengths. This is because the thrust shared by the pile increases. However, the axial force of anchor cables at the leading edge and the trailing edge of the slope remains almost unchanged. This indicates that piles hardly have an effect on anchor cables in front of the piles or at the trailing edge of the slope.

Figure 21 also shows that there is a significant change in the axial force of the anchor cable as the pile length increases from 20 to 35 m. However, this change is not significant when the pile length increases from 35 to 40 m. This is because the proportion of thrust shared by the piles and anchor cables remains almost constant when the embedded length of the piles is greater than 1/3 of the total length, as shown in Fig. 22.

Similar results can be seen in Yang et al. (2011), Xu and Huang (2021), and Wang et al. (2021a, b). They pointed out that the excessive embedment length of the pile is redundant and there is a critical length. Additionally, the

**Fig. 20** Diagram of internal force of piles for different pile lengths: (1) bending moment and (2) shear force



**Fig. 21** Axial force of anchor cables for different pile lengths

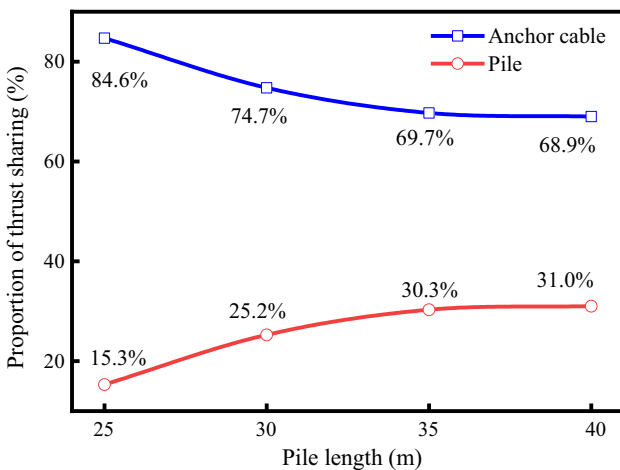


**Fig. 22** Proportion of the thrust shared by piles and anchor cables for different pile lengths

**Table 6** Calculation schemes for different pile spacing

Scheme	Pile position	Pile length (m)	Pile spacing (m)
1	Pile 1	40	4
2	Pile 1	40	5
3	Pile 1	40	6
4	Pile 1	40	7

specification (DZ/T 0219-2006) recommends an embedment length of 1/3–2/5 of the total length of the pile. Thus, 1/3 of the total length can be adopted as the optimal embedded length of piles considering the economics of projects.

**Effect of pile spacing**

Four different pile spacing were considered, as shown in Table 6. To determine the critical values of pile spacing, a wide range of the parameter is initially selected referring to the Code for the design of landslide stabilization (GB/T 38509-2020). The pile spacing was set to 4 m, 5 m, 6 m, and 7 m, respectively. Other parameters remain unchanged.

**Stability of slope**

Figure 23 shows the equivalent plastic strain contours of the slope for different pile spacing. For the pile spacing of 4 m and 5 m, the soil in front of the pile shows plastic deformation upwards with the pile, whereas for the pile spacing of 6 m and 7 m, plastic deformation occurs only near the slip surface. This indicates that the pile exerts

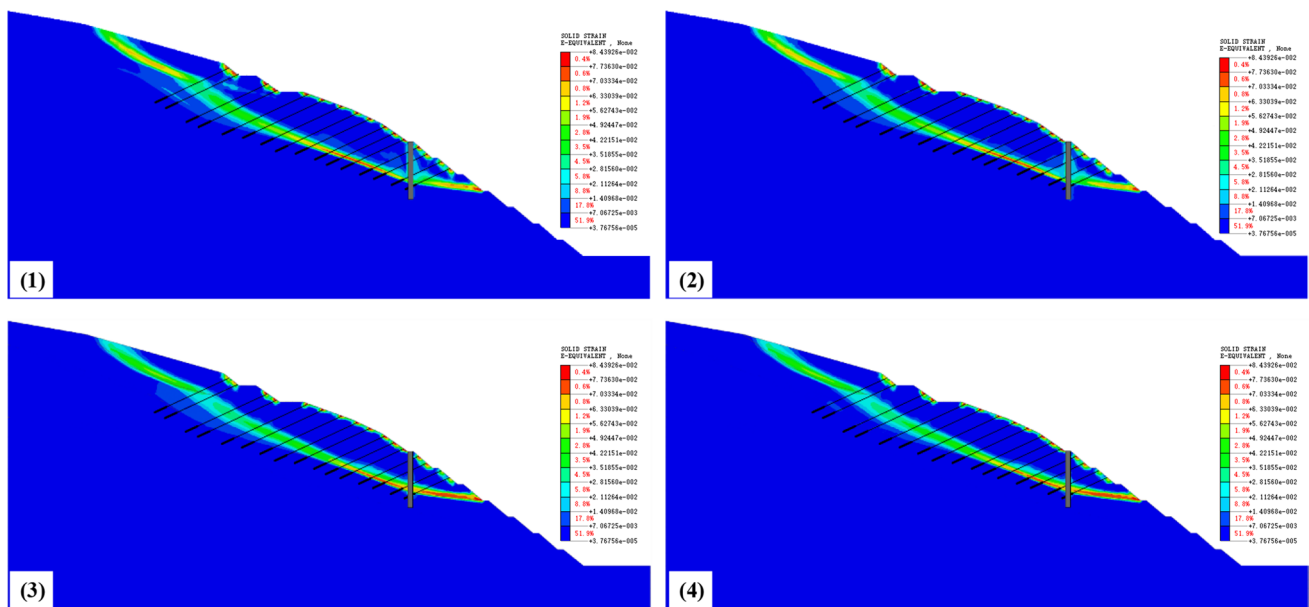


**Fig. 23** Equivalent plastic strain contours of slopes for different pile spacing: (1) 4 m; (2) 5 m; (3) 6 m; and (4) 7 m

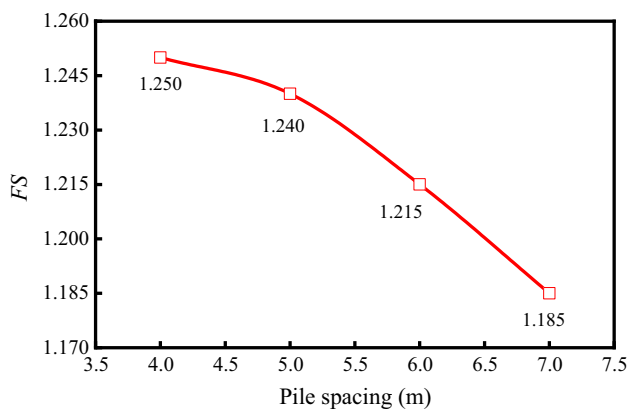


**Fig. 24** FS of slopes for different pile spacing

more thrust on the soil in front of the pile for the pile spacing less than 5 m; conversely, it is difficult for the pile to exert thrust on the soil in front of the pile for the pile spacing greater than 5 m.

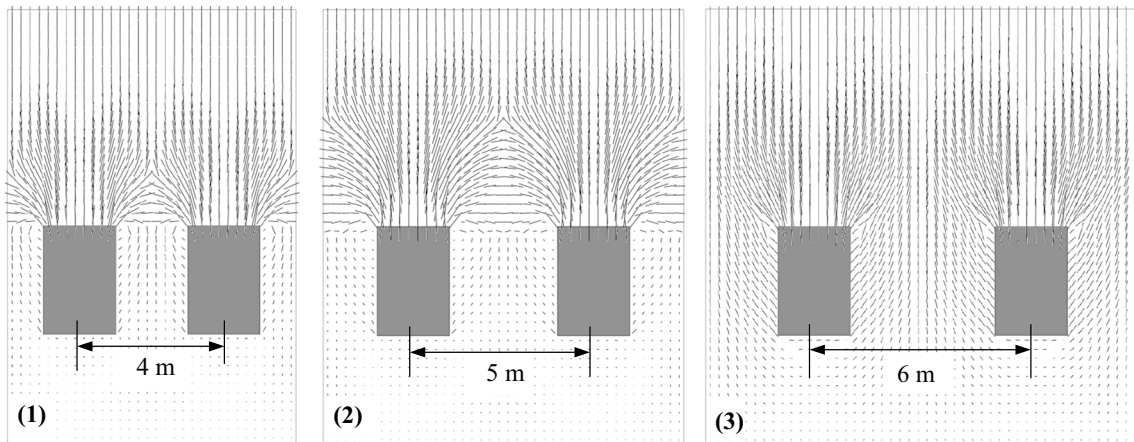
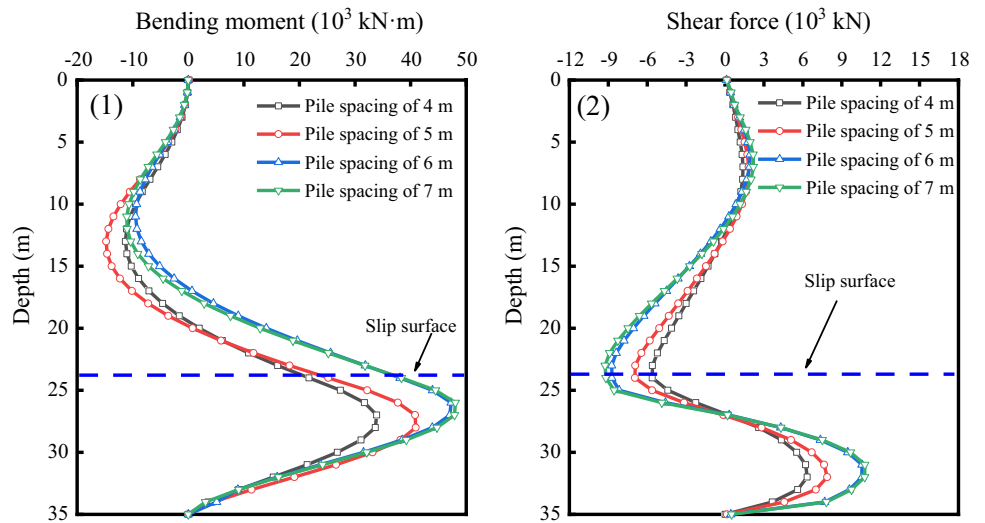
Figure 24 shows the FS of slopes for different pile spacing. The FS of the slope for the pile spacing of 4 m is 1.250. The FS gradually decreases with the increased pile spacing. Compared to the pile spacing of 4 m, the FS of the slope for pile spacings of 5 m, 6 m, and 7 m is decreased by 0.8%, 2.8%, and 5.2%, respectively. In addition, the change rate of the FS for the pile spacing of 4–5 m is less than the rate of 5–7 m. This indicates that the stability of the slope decreases rapidly after the pile spacing exceeds 5 m.

### Internal force of piles and axial force of anchor cables

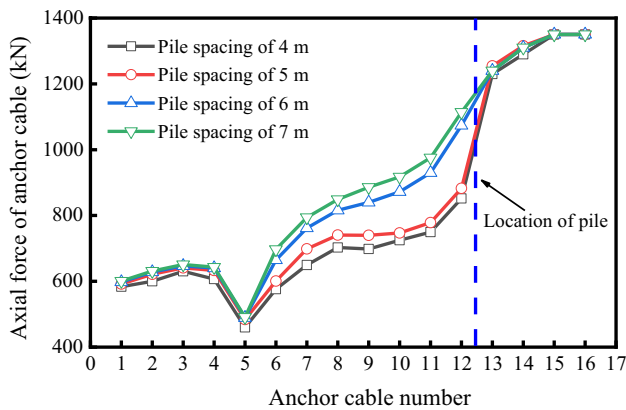
Figure 25 shows the diagram of bending moment and shear force of piles for different pile spacing. The shapes of the bending moments and the shear forces hardly change for different pile spacing. However, the value of the bending moments and the shear forces increase with the increased pile spacing, which is in agreement with the results from Yang et al. (2011). This can be explained by the fact that the soil’s width affected by a single pile increases and shares more of the landslide thrust with the increased pile spacing.

Figure 25 also shows that the bending moment and shear force do not change uniformly with the increased pile spacing, which may be related to the soil arch effect between the piles. Figure 26 shows the vector diagram of the principal stress of the soil around the pile for different pile spacing. The principal stress vector clearly shows an arch shape and the principal stress vector is significantly deflected between piles for the pile spacing of 4 m and 5 m. The soil arch effect disappears for the pile spacing increases to 6–7 m, which indicates that the effective soil arch cannot be formed if the pile spacing exceeds 5 m (2.5 times the width of the pile section). This is in agreement with the critical pile spacing of 2.7 times the pile diameter derived by Ellis et al. (2010). Additionally, it is important to note that the critical pile spacing is also related to the properties of the soil (Wei and Cheng 2009; Yang et al. 2011). The pile spacing may be increased for soils with better properties.

**Fig. 25** Diagram of internal force of piles for different pile spacing: (1) bending moment and (2) shear force



**Fig. 26** Vector diagram of the principal stress of the soil around the pile for different pile spacing: (1) 4 m; (2) 5 m; and (3) 6 m



**Fig. 27** Axial force of anchor cables for different pile spacing

Figure 27 shows the axial force of anchor cables for different pile spacing. The axial force of the anchor cables in the middle of the slope increases with the increased pile spacing. This is because the weakened soil arch between the piles reduces the thrust shared by the piles and increases the thrust shared by the anchor cables. This mechanism can also be confirmed by the proportion of thrust shared by the anchor cable and the pile, as shown in Fig. 28. However, the axial forces of the anchor cables at the leading edge and the trailing edge of the slope do not change significantly with the pile spacing. The reason is similar to the effect of pile length on the axial force of anchor cables "Effect of pile length".

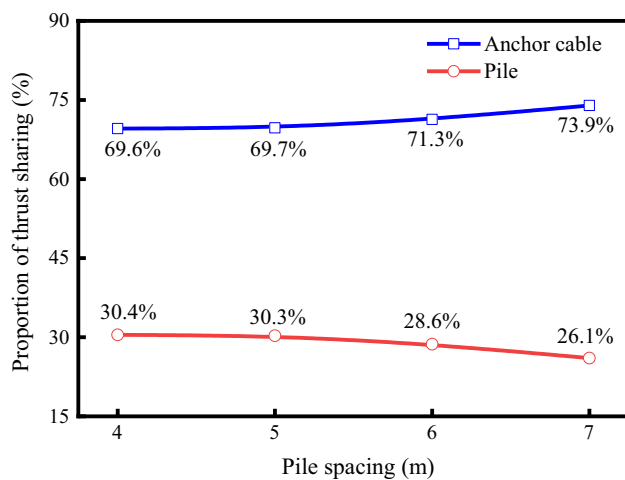


**Fig. 28** Proportion of the thrust shared by piles and anchor cables for different pile spacing

## Conclusions

In this study, detailed work has been done on a landslide. A series of numerical models of the slope stabilized with piles and anchor cable frame beams were developed using a three-dimensional finite-element method. The Strength Reduction Method was employed to investigate the stability of slopes, the internal forces of piles, and the axial forces of anchor cables. A parametric study consisting of pile position, pile length, and pile spacing was carried out. The following main conclusions were drawn.

1. Compared to anchor cable frame beams, the combination of piles and anchor cable frame beams is a more effective retaining structure to improve slope stability. The proportion of thrust shared by piles gradually increases, while the proportion of thrust shared by anchor cables gradually decreases during slope destabilization.
2. Piles installed on the leading edge of a trail-mode landslide can make the slope mostly stable. As the piles move from the leading, middle, and trailing edges of the slope, the proportion of thrust shared by the anchor cables gradually increases, while local instability may occur in front of the pile.
3. Increasing the pile length can improve the stability of the slope. However, excessive embedded length of piles has little effect on further improving the slope stability. The critical embedment length of piles found in this study is 1/3 of the total length of the pile.
4. The critical pile spacing found in this study is 2.5 times the width of the pile section. Beyond this spacing, the effective soil arch between the piles is difficult to develop and the anchor cables may share more proportion of the landslide thrust.

**Acknowledgements** The support from the National Key Research and Development Program of China (Grant no. 2019YFC1509700) is gratefully acknowledged. The third author has provided great help in writing and revising this study.

**Author contributions** CD: writing—original draft, calculation, and analysis; JC: methodology, supervision, and funding acquisition; SC: conceptualization, methodology, review, and editing; MP: supervision, writing—review and editing, funding acquisition, and resources; ZS: review and editing, and resources.

**Data availability** The data that support the findings of this study are available from the corresponding author upon reasonable request.

## Declarations

**Conflict of interest** The authors have no relevant financial or nonfinancial interests to disclose.

## References

- Arvin MR, Zakeri A, Bahmani Shoorijeh M (2019) Using finite element strength reduction method for stability analysis of geocell-reinforced slopes. *Geotech Geol Eng* 37(3):1453–1467. <https://doi.org/10.1007/s10706-018-0699-0>
- Bo Z, Yun W, Yu W, Tong S, Yong Z (2017) Retaining mechanism and structural characteristics of h type anti-slide pile (hTP pile) and experience with its engineering application. *Eng Geol* 222:29–37. <https://doi.org/10.1016/j.enggeo.2017.03.018>
- Cai F, Ugai K (2000) Numerical analysis of the stability of a slope stabilized with piles. *Soils Found* 40(1):73–84. <https://doi.org/10.3208/sandf.40.73>
- Chen Z, Wang Z, Xi H, Yang Z, Zou L, Zhou Z, Zhou C (2016) Recent advances in high slope reinforcement in China: case studies. *J Rock Mech Geotech Eng* 8(6):775–788. <https://doi.org/10.1016/j.jrmge.2016.11.001>
- Chen G, Chen T, Chen Y, Huang R, Liu M (2018) A new method of predicting the prestress variations in anchored cables with excavation unloading destruction. *Eng Geol* 241:109–120. <https://doi.org/10.1016/j.enggeo.2018.05.015>
- DZ/T 0219-2006. Specification of design and construction for landslide stabilization. In: National Standard of the People's Republic of China in the Field of Geology and Mineral Resources. Ministry of Land and Resources of the People's Republic of China Press, Beijing (**in Chinese**)
- Ellis E, Durrani I, Reddish D (2010) Numerical modeling of discrete pile rows for slope stability and generic guidance for design. *Geotechnique* 60(3):185–195. <https://doi.org/10.1680/geot.7.00090>
- Feng SJ, Fu WD, Chen HX, Li HX, Xie YL, Lv SF, Li J (2021) Field tests of micro screw anchor piles under different loading conditions at three soil sites. *B Eng Geol Environ* 80(1):127–144. <https://doi.org/10.1007/s10064-020-01956-y>
- GB/T 38509-2020. Code for the design of landslide stabilization. State Administration for Market Regulation (**in Chinese**)
- Griffiths DV, Marquez RM (2007) Three-dimensional slope stability analysis by elasto-plastic finite elements. *Geotechnique* 57(6):537–546. <https://doi.org/10.1680/geot.2007.57.6.537>
- Hassiotis S, Chameau JL, Gunaratne M (1997) Design method for stabilization of slopes with piles. *J Geotech Geo-Environ* 123(4):314–323. [https://doi.org/10.1061/\(ASCE\)1090-0241\(1997\)123:4\(314\)](https://doi.org/10.1061/(ASCE)1090-0241(1997)123:4(314))

- Ito T, Matsui T, Hong WP (1981) Design method for stabilizing piles against landslide—one row of piles. *Soils Found* 21(1):21–37. <https://doi.org/10.3208/sandf1972.21.21>
- Kahyaoglu MR, İmançlı G, Özden G, Kayalar AŞ (2017) Numerical simulations of landslide-stabilizing piles: a remediation project in Söke, Turkey. *Environ Earth Sci* 76(19):1–14. <https://doi.org/10.1007/s12665-017-6989-7>
- Kang GC, Song YS, Kim TH (2009) Behavior and stability of a large-scale cut slope considering reinforcement stages. *Landslides* 6(3):263–272. <https://doi.org/10.1007/s10346-009-0164-5>
- Li H, Du QW (2021) Stabilizing a post-landslide loess slope with anti-slide piles in Yan'an. *China Environ Earth Sci* 80(22):1–13. <https://doi.org/10.1007/s12665-021-10051-8>
- Li DF, Wang LJ (2016) Synergism analysis of bedding slope with piles and anchor cable support under sine wave vehicle load. *Ad Mat Sci Eng* 2016:1–8. <https://doi.org/10.1155/2016/5753970>
- Li C, Wu J, Tang H, Hu X, Liu X, Wang C, Zhang Y (2016) Model testing of the response of stabilizing piles in landslides with upper hard and lower weak bedrock. *Eng Geol* 204:65–76. <https://doi.org/10.1016/j.enggeo.2016.02.002>
- Li C, Yan J, Wu J, Lei G, Wang L, Zhang Y (2019) Determination of the embedded length of stabilizing piles in colluvial landslides with upper hard and lower weak bedrock based on the deformation control principle. *B Eng Geol Environ* 78(2):1189–1208. <https://doi.org/10.1007/s10064-017-1123-3>
- Lin H, Xiong W, Cao P (2013) Stability of soil nailed slope using strength reduction method. *Eur J Environ Civil Eng* 17(9):872–885. <https://doi.org/10.1080/19648189.2013.828658>
- Lin YL, Li YX, Yang GL, Li Y (2017) Experimental and numerical study on the seismic behavior of anchoring frame beam supporting soil slope on rock mass. *Soil Dyn Earthq Eng* 98:12–23. <https://doi.org/10.1016/j.soildyn.2017.04.008>
- Liu XR, Kou MM, Feng H, Zhou Y (2018) Experimental and numerical studies on the deformation response and retaining mechanism of h-type anti-sliding piles in clay landslide. *Environ Earth Sci* 77(5):1–14. <https://doi.org/10.1007/s12665-018-7360-3>
- Poulos HG (1995) Design of reinforcing piles to increase slope stability. *Can Geotech J* 32(5):808–818. <https://doi.org/10.1139/t95-078>
- Rawat S, Gupta AK (2016) Analysis of a nailed soil slope using limit equilibrium and finite element methods. *Int J Geosynth Ground Eng* 2(4):34. <https://doi.org/10.1007/s40891-016-0076-0>
- Shooshpasha I, Amirdehi HA (2015) Evaluating the stability of slope stabilized with one row of free head piles. *Arab J Geosci* 8(4):2131–2141. <https://doi.org/10.1007/s12517-014-1272-7>
- Tan Q, Tang H, Huang L, Li C, Kou T (2018) LSP methodology for determining the optimal stabilizing pile location for step-shaped soil sliding. *Eng Geol* 232:56–67. <https://doi.org/10.1016/j.enggeo.2017.11.005>
- Wang J, Nie Z, Liu J, Qin M, Rongzi OU (2021a) Analysis of fracture reliability of anti-slide deep pile reinforced slope under flood effect. *Environ Earth Sci* 80(16):1–12. <https://doi.org/10.1007/s12665-021-09834-w>
- Wang C, Wang H, Qin W (2021b) Experimental and numerical studies on the behavior and retaining mechanism of anchored stabilizing piles in landslides. *B Eng Geol Environ* 80(10):7507–7524. <https://doi.org/10.1007/s10064-021-02391-3>
- Wei WB, Cheng YM (2009) Strength reduction analysis for slope stabilized with one row of piles. *Comput Geotech* 36(7):1176–1185. <https://doi.org/10.1016/j.compgeo.2009.05.004>
- Wu LZ, Huang RQ (2008) Calculation of the internal forces and numerical simulation of the anchor frame beam strengthening expansive soil slope. *Geotech Geol Eng* 26(5):493–502. <https://doi.org/10.1007/s10706-008-9184-5>
- Xiao SG (2017) A simplified approach for stability analysis of slopes reinforced with one row of embedded stabilizing piles. *B Eng Geol Environ* 76(4):1371–1382. <https://doi.org/10.1007/s10064-016-0934-y>
- Xiao S, Zeng J, Yan Y (2017) A rational layout of double-row stabilizing piles for large-scale landslide control. *B Eng Geol Environ* 76(1):309–321. <https://doi.org/10.1007/s10064-016-0852-z>
- Xu X, Huang Y (2021) Parametric study of structural parameters affecting seismic stability in slopes reinforced by pile-anchor structures. *Soil Dyn Earthq Eng* 147:106789. <https://doi.org/10.1016/j.soildyn.2021.106789>
- Xue D, Li T, Zhang S, Ma C, Gao M, Liu J (2018) Failure mechanism and stabilization of a basalt rock slide with weak layers. *Eng Geol* 233:213–224. <https://doi.org/10.1016/j.enggeo.2017.12.005>
- Yang S, Ren X, Zhang J (2011) Study on embedded length of piles for slope reinforced with one row of piles. *J Rock Mech Geotech Eng* 3(2):167–178. <https://doi.org/10.3724/SP.J.1235.2011.00167>
- Zhang Y, Zhang Z, Xue S, Wang R, Xiao M (2020) Stability analysis of a typical landslide mass in the Three Gorges Reservoir under varying reservoir water levels. *Environ Earth Sci* 79(1):1–14. <https://doi.org/10.1007/s12665-019-8779-x>
- Zhao B, Wang YS, Wang Y, Shen T, Zhai YC (2017) Retaining mechanism and structural characteristics of h type anti-slide pile (hTP pile) and experience with its engineering application. *Eng Geol* 222:29–37. <https://doi.org/10.1016/j.enggeo.2017.03.018>
- Zhao G, Yang Y, Zhang H, Zhang G (2019) A case study integrating field measurements and numerical analysis of high-fill slope stabilized with cast-in-place piles in Yunnan, China. *Eng Geol* 253:160–170. <https://doi.org/10.1016/j.enggeo.2019.03.005>

**Publisher's Note** Springer Nature remains neutral with regard to jurisdictional claims in published maps and institutional affiliations.

Springer Nature or its licensor (e.g. a society or other partner) holds exclusive rights to this article under a publishing agreement with the author(s) or other rightsholder(s); author self-archiving of the accepted manuscript version of this article is solely governed by the terms of such publishing agreement and applicable law.